Reconstructing marine productivity of the Cariaco Basin during marine isotope stages 3 and 4 using organic-walled dinoflagellate cysts

Catalina González,[1] Lydie M. Dupont,[1] Kenneth Mertens,[2] and Gerold Wefer[1]

[1] An organic-walled dinoflagellate cyst analysis was carried out on sediment core MD03-2622, retrieved from the Cariaco Basin. The core comprises the 73–30 ka interval. Down core changes in cyst abundance, accumulation rate, and composition of cyst assemblages were used to identify climatic and oceanographic changes at orbital and millennial time scales in this near-equatorial seasonal upwelling area. Throughout the sequence, dinoflagellate cyst assemblages were dominated by heterotrophic dinocysts (mainly *Brigantedinium* spp.), with the exception of four autotrophic-dominated (mainly *Spiniferites ramosus*) intervals around 58, 53, 46, and 37 ka. At orbital time scales, changes in the dinoflagellate productivity seem to follow low-latitude insolation, with the highest productivities coinciding with maximum February insolation (47–38 ka). At millennial scales, cyst accumulation rates appeared to coincide with Dansgaard-Oeschger (D-O) variability, with significant increments occurring during warm interstadials. The opposite was true during stadials. Short periods of high nutrient availability and stratified conditions followed Heinrich events H4, H5, H5a, and H6 and concurred with enhanced river runoff. Spectral analyses confirm the existence of these and other higher-frequency periodicities and support the idea of a tightly coupled terrestrial/marine and tropical/high-latitude climate system during the last glacial period.

1. Introduction

[2] Marine eukaryotic production is an important factor in the climate system as it contributes to changing atmospheric CO_2 through biological fixing and export of organic carbon to the deep sea. Studies on paleoproductivity are therefore important because they place constraints on past ocean circulation, nutrient distribution and on the history of the oceanic carbon cycle. In spite of the significant role that the Caribbean Sea plays in the heat and mass transport from the tropics to higher latitudes [e.g., *Gordon*, 1967; *Metcalf*, 1976; *Mooers and Maul*, 1998; *Schmidt et al.*, 2004], studies on late Quaternary paleoproductivity in this region are scarce [*J. I. Martinez et al.*, 2007; *Kameo et al.*, 2004]. The Caribbean Sea is generally characterized by nutrient-depleted surface waters. However, in its southernmost part, coastal upwelling and river discharge of South American rivers promote nutrient-rich waters [*Muller-Karger et al.*, 2004].

[3] The Cariaco Basin, on the continental shelf of Venezuela, besides undergoing marked seasonal upwelling, is an important source of palaeoclimatic information [e.g., *Peterson et al.*, 1991, 2000a; *Hughen et al.*, 1996, 2004b; *Haug et al.*, 2001]. Previously published records from the Cariaco Basin have provided valuable information on the marine productivity history of the region. Extensive information exists for the past 16 ka. For example, *Peterson et al.* [1991], *Hughen et al.* [1996], and *Werne et al.* [2000] observed that the Younger Dryas marked the onset of a period of strong upwelling, coinciding with strong meridional sea surface temperature (SST) gradients in the Atlantic and the consequent intensification of trade winds. More recently, *Dahl et al.* [2004] characterized the assemblages of the phytoplankton community through the same period using biomarkers, and found important differences between the strong upwelling interval (diatom-dominated) and the Bølling/Allerød warm period (dinoflagellate-dominated). At longer time scales, direct evidence of productivity variations in the Cariaco Basin has been derived from $CaCO_3$ fluxes [*Peterson et al.*, 2000a] and alkenone concentration records [*Herbert and Schuffert*, 2000]. However, these records only provide insight into the paleoproductivity of the calcareous surface plankton, and thus can be potentially problematic, since carbonate dissolution might have affected the paleoenvironmental signal. Moreover, the existing records are not long enough, as in case of the $CaCO_3$ record, or not detailed enough, as in case of the alkenone record, to resolve the millennial-scale variability of marine productivity over marine isotope stage (MIS) 3, particularly during the Heinrich events (HEs) from the North Atlantic [*Bond et al.*, 1992, 1997; *Dansgaard et al.*, 1993].

[4] The analysis of organic-walled dinoflagellate cyst (dinocysts for short) in marine sediments has become a valuable tool to obtain reconstructions of past eukaryotic

[1]MARUM, University of Bremen, Bremen, Germany.
[2]Research Unit Palaeontology, Department of Geology and Soil Science, Ghent University, Ghent, Belgium.
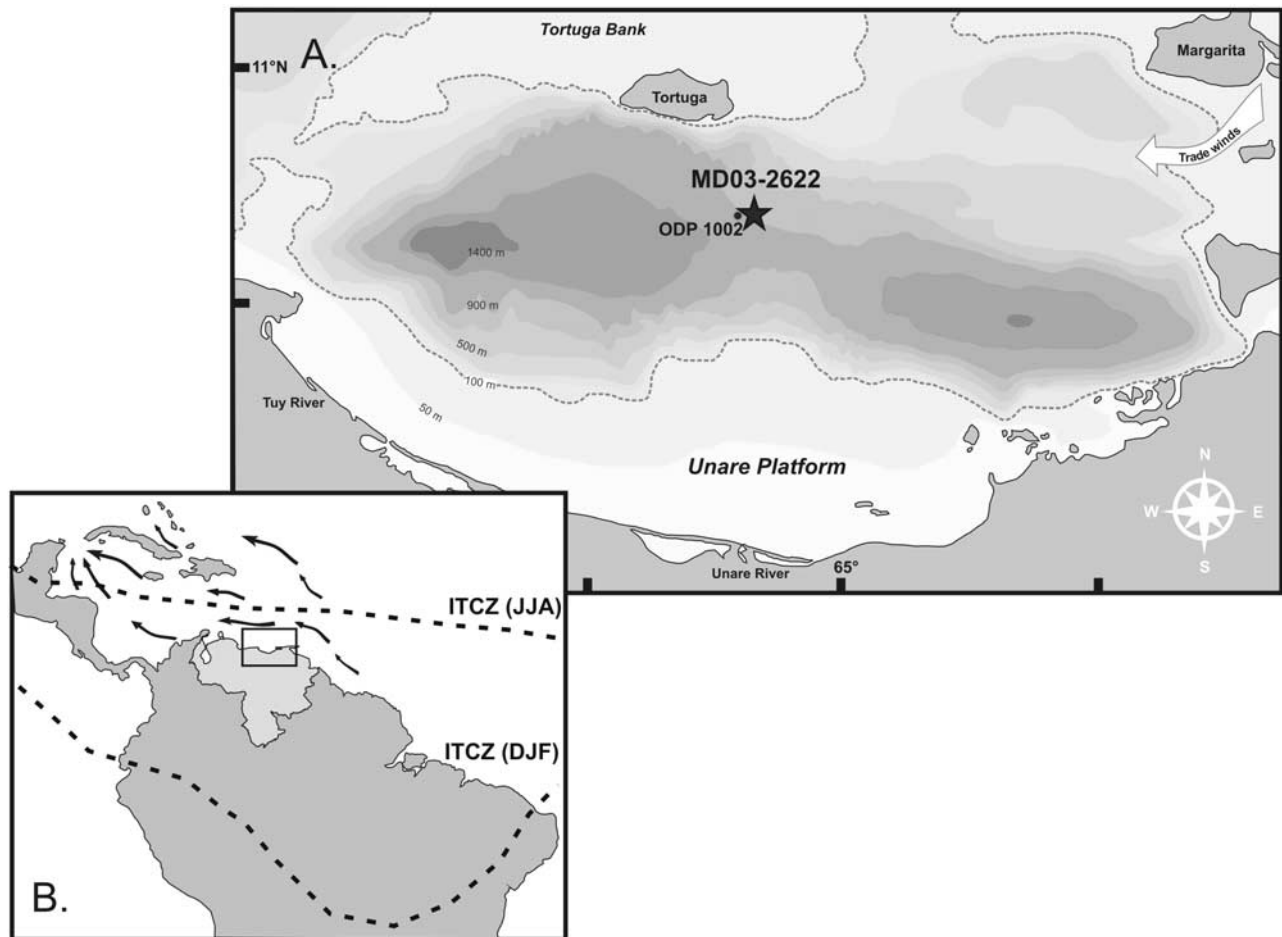
Figure 1. Maps of the study area. (a) The Cariaco Basin, bathymetry and location of core MD03-2622 (star) and ODP site 1002 (black circle). (b) Yearly migration of the Intertropical Convergence Zone (ITCZ) over northern South America. Modern latitudinal limits are denoted as dotted lines. Arrows show the main surface circulation pattern in the Caribbean.

productivity in the oceans, especially in highly productive environments, in which carbonate dissolution constitutes a major problem [*Berger et al.*, 1982]. It has been shown that the spatial and seasonal distribution of dinocysts correlate with physical sea surface conditions (e.g., temperature, salinity, nutrients, and light penetration) [*Wall et al.*, 1977; *de Vernal et al.*, 2001; *Marret and Zonneveld*, 2003, and references therein]. The resistant organic walls of dinocysts are generally well preserved in the sediments, and thus, the dinocyst distributions in marine cores can be used to infer physical characteristics of past sea surface. In coastal and neritic settings, dinocysts exhibit particularly high abundances, and thus they constitute a suitable proxy to complement the paleoenvironmental information derived from typically marine groups such as coccolithophorids, diatoms, and planktonic foraminifera. In spite of the ecological importance of dinoflagellates as main constituents of the marine primary producers [*Parsons et al.*, 1984], understanding of dinocyst distribution in upwelling areas is still insufficient.

[5] Therefore, in the following contribution we present new high-resolution dinocyst data, providing new insights into the history of eukaryotic productivity in a tropical upwelling region during MIS 3 and 4 (73–30 ka). We document variations in dinoflagellate species composition, relative cyst abundances, and accumulation rates at centennial-millennial intervals, in order to address how marine productivity changed in the Cariaco Basin in relation to past rapid climatic changes.

2. Cariaco Basin: Environmental Setting and Background

[6] The Cariaco Basin is located on the northern shelf of Venezuela (Figure 1). Today, anoxia occurs below ∼300 m as a result of the high seasonal productivity, and the shallow sills (∼ 150 m depth) that restrict horizontal water exchange with the rest of the Caribbean and the large river plumes from the Orinoco and Amazon [*Muller-Karger et al.*, 2004].

[7] Because of its northern equatorial position, the Cariaco Basin is particularly sensitive to seasonal and long-scale fluctuations in the latitudinal position of the Intertropical Convergence Zone (ITCZ). During the Northern Hemisphere

winter (January–March), trade winds blow along the northern coast of South America inducing upwelling [*Muller-Karger et al.*, 2001]. Seasonal upwelling is directly linked to lower SST (22°C) and higher sea surface salinity (SSS; 36.8 psu). During this season, primary productivity reaches its maximum and the phytoplankton community is dominated mainly by diatoms, and a minor proportion of heterotrophic dinoflagellates [*Ferraz-Reyes*, 1983]. During unusually weak upwelling seasons, possibly related to El Niño, haptophyte algae have been reported to prevail over diatoms [*Goñi et al.*, 2003]. A contrasting rainy season develops over the Cariaco Basin during the late boreal summer and early autumn, when the ITCZ is directly overhead and rainfall reaches its maximum, causing trade winds and upwelling in the basin to diminish. A relatively fresh layer develops at the surface (36.3 psu) and stratified conditions coincide with maximum SST (28.5°C). Primary production during the nonupwelling season is lower [*Muller-Karger et al.*, 2001] and a more diverse phytoplankton community develops, mostly composed of dinoflagellates and cyanobacteria. Coastal assemblages are relatively better developed during the rainy season as they benefit from the fluvial discharge of fresh water and nutrients [*Ferraz-Reyes*, 1983]. Because of the anoxic bottom water conditions on the Cariaco Basin, the absence of bioturbation, and the high sedimentation rates (30–100 cm/ka), this annual migration of the ITCZ is preserved in the Cariaco Basin sediment as an intermitent accumulation of seasonal laminae, which are ideal for paleoclimatic reconstructions.

[8] At interannual scales the Atlantic ITCZ is affected by the El Niño–Southern Oscillation (ENSO) and the North Atlantic subtropical high sea level pressure system [*Giannini et al.*, 2000]. ENSO events cause atmospheric circulation anomalies over the Tropics, thus having a direct effect on precipitation variability [*Giannini et al.*, 2001]. Warm phases of ENSO (El Niño) are characterized by below-average rainfall over the Caribbean/Central American region, opposite to cold ENSO events (La Niña) that are related to positive rainfall anomalies. Furthermore, occasional lower phytoplankton production in the Cariaco Basin might be related to warm ENSO events [*Muller-Karger et al.*, 2004].

[9] Throughout the Late Quaternary, the Cariaco Basin is distinguished by an alternation between periods of oxic and anoxic conditions, related to glacial-interglacial cycles, that are reflected in the sequence as fluctuations between bioturbated (oxic) and laminated (anoxic) sediments [*Peterson et al.*, 2000b]. Analogous to the seasonal migrations of the ITCZ, longer-term (e.g., orbital-scale, millennial-scale) changes in the mean position of the ITCZ have been proposed as the most probable mechanism linking northern high-latitude and tropical climates [*Peterson and Haug*, 2006] that eventually might have caused changes in primary productivity and phytoplankton community structure in the Cariaco Basin [*Haug et al.*, 1998].

[10] Terrigenous material is deposited into the Cariaco Basin via fluvial and aeolian pathways. Sea level has modulated the relative contribution of sediments of major and minor local rivers during interglacial highstands and glacial lowstands. During glacial periods, e.g., MIS 3 and MIS 4, sea level was ~80–120 m below present level [*Lambeck and Chappell*, 2001; *Siddall et al.*, 2003], the sills surrounding the basin became shallower, and the basin was mostly isolated from sediments derived from the Amazon and Orinoco Rivers. Local rivers (Manzanares, Neverí, Unare and Tuy Rivers) that drain the northern coastline of Venezuela, on the other hand, were more proximal to the edge of the basin and became volumetrically more important. Al/Ti and K/Ti ratios in bulk sediment [*Yarincik et al.*, 2000] and clay mineralogy [*Clayton et al.*, 1999] from the Cariaco Basin show that its sediment imprint greatly differs from that of the Amazon and Orinoco Rivers, as during glacial periods the input of terrigenous sediments mainly records the input from local rivers and Saharan derived eolian matter [*N. C. Martinez et al.*, 2007].

[11] African aeolian sediment, specifically dust from the Sahara and Sahel regions, has been traced over the tropical Atlantic all the way to the Caribbean [*Prospero and Lamb*, 2003], and its contribution has been estimated to be no more than a few percent of the total terrigenous input. It has been suggested that during glacials, maximum dust input coming from Africa reached the western equatorial Atlantic [*Yarincik et al.*, 2000; *N. C. Martinez et al.*, 2007].

3. Materials and Methods

[12] Marine calypso core MD03-2622 (10°42.69′ N; 65°10.15′ W; 877 m water depth), was retrieved during P.I.C.A.S.S.O cruise in 2003 [*Laj*, 2004], proximate to the location of Ocean Drilling Program Site 1002 on the western edge of the central saddle of the Cariaco Basin (Figure 1). The chronology used in this study was developed by correlating the reflectance curve of core MD03-2622 with the reflectance of core ODP 1002D [*Peterson et al.*, 2000a, Figure 1], which has an extremely high-resolution age model for the past 60 ka based on AMS ^{14}C data on planktic foraminifera [*Hughen et al.*, 2004a, 2006], and was subsequently tied to that of the independently ^{230}Th-dated Hulu Cave stalagmites [*Wang et al.*, 2001].

[13] For the period comprising MIS 3 and 4 (73–30 ka, 1ka = 1000 years BP), the core was sampled at 15 cm intervals, resulting in an average temporal resolution of ~300 years, and at 2 cm intervals for the period corresponding to interstadial 8 (38.4–36.4 ka) resulting in an average temporal resolution of ~50 years. Around 150 samples were prepared for organic-walled dinocyst analysis using standard laboratory methods, which include decalcification with HCl (~10%) and subsequent removal of silicates with HF (~20%). Two *Lycopodium clavatum* tablets, containing a known number of spores, were added during the decalcification process. After neutralization with KOH and washing, the samples were sieved with ultrasound over a 8 μm nylon mesh during ~60 s to remove particles < 10μm. Permanent slides were mounted in a gelatin-glycerin medium for microscopic examination. Dinoflagellate cysts were counted up to 300 specimens. Simultaneously, *Lycopodium* spores counts were attained for calculation of dinoflagellate cysts concentration (cysts/cm^3) based on the proportion of exotic *Lycopodium* spores counted to the initial number of *Lycopodium* spores added [*Maher*, 1981]. Accumulation

Table 1. List of Identified Organic-Walled Dinoflagellate Cysts Taxa From Site MD03-2622, Cariaco Basin

Identified Cysts	Motile Affinity [*Marret and Zonneveld*, 2003]
Bitectatodinium spongium (Zonneveld, 1997) Zonneveld and Jurkschat	unknown
Brigantedinium cariacoense (Wall) Lentin and Williams	*Protoperidinium avellanum*
Brigantedinium sp.	*Protoperidinium* spp.
Echinidinium aculeatum Zonneveld	Protoperidinoid
Echinidinium delicatum Zonneveld	Protoperidinoid
Echinidinium spp.	Protoperidinoid
Echinidinium T.1	Protoperidinoid
Echinidinium T.2	Protoperidinoid
Echinidinium cf. *transparantum* Zonneveld	Protoperidinoid
Impagidinium aculeatum (Wall) Lentin and Williams	*Gonyaulax* sp. Indet.
Impagidinium plicatum Versteegh and Zevenboom	*Gonyaulax* sp. Indet.
Impagidinium sphaericum (Wall) Lentin and Williams	*Gonyaulax* sp. Indet.
Impagidinium strialatum (Wall) Stover and Evitt	*Gonyaulax* sp. Indet.
Impagidinium T.1	*Gonyaulax* sp. Indet.
Islandinium cf. *minutum* (Harland and Reid in Harland et al.)	*Protoperidinium* sp. Indet.
Leipokatium invisitatum Bradford	Protoperidinoid
Lejeunecysta oliva (Reid) Turon and Londeix	*Protoperidinium* sp. Indet.
Lejeunecysta sabrina (Reid) Bujak	*Protoperidinium leone*
Lingulodinium machaerophorum (Deflandre and Cookson) Wall	*Lingulodinium polyedrum*
Nematosphaeropsis labyrinthus (Ostenfeld) Reid	*Gonyaulax spinifera* complex
Operculodinium centrocarpum sensu Wall and Dale	*Protoceratium reticulatum*
Operculodinium israelianum (Rossignol) Wall	*Protoceratium* sp.?
Cyst of *Pentapharsodinium dalei* Indelicato and Loeblich III	*Pentapharsodinium dalei*
Quinquecuspis concreta (Reid) Harland	*Protoperidinium leone*
Selenopemphix cf. *divaricatum*	Protoperidinoid
Selenopemphix nephroides Benedek emend, Bujak	*Protoperidinium subinerme*
Selenopemphix quanta (Bradford) Matsuoka	*Protoperidinium conicum*, *P. nudum*
Spiniferites cf. *bentorii* (Rossignol) Wall and Dale	*Gonyaulax digitalis*
Spiniferites hyperacanthus (Deflandre and Cookson) Cookson and Eisenack	*Gonyaulax spinifera* complex
Spiniferites membranaceus (Rossignol) Sarjeant	*Gonyaulax spinifera* complex
Spiniferites mirabilis (Rossignol) Sarjeant	*Gonyaulax spinifera* complex
Spiniferites pachydermus (Rossignol) Reid	*Gonyaulax* sp. Indet.
Spiniferites ramosus (Ehrenberg) Mantell sensu lato	*Gonyaulax spinifera* complex
Spiniferites spp.	*Gonyaulax spinifera* complex
Stelladinium reidii Bradford	*Protoperidinium stellatum*
Tuberculodinium vacampoae (Rossignol) Wall	*Pyrophacus steinii*
Votadinium calvum Reid 1977	*Protoperidinium oblongum*

rates (cysts/cm^2/a) were calculated by multiplying the palynomorph concentration by the sedimentation rate (cm/a). Pollen data for comparison come from the same set of samples [*González et al.*, 2008]. Assemblages (expressed in relative abundances), dinocysts concentrations and accumulation rates of were plotted versus age.

[14] Identification of main cyst types was based on published morphological descriptions [*Rochon et al.*, 1999; *Marret and Zonneveld*, 2003]. Before statistical treatment, some dinoflagellate cysts that could not be identified to species level were grouped. *Brigantedinium* spp. includes all round brown specimens (e.g., *Brigantedinium cariacoense* and *B. simplex*); *Echinidinium* spp., contains all *Echinidinium* cysts except for *E. aculeatum* and *E. delicatum*, and *Spiniferites* spp. comprises all nonidentifiable *Spiniferites*.

[15] Spectral analysis and wavelet analysis were performed on dinoflagellate cyst accumulation rates and relative abundances. Time series were previously detrended by removing the cubic trend, and then normalized to unit variance. Additionally, they were evenly resampled by integrating between points using a linear function, in order to obtain a uniform 200 year interval, which is close to the original mean temporal resolution. The employed Blackman-Tuckey (B-T) spectral analysis method makes it unlikely to

present spurious spectral features, although it has a relatively poor resolution in the spectral domain. B-T analyses were performed using AnalySeries 1.1 software [*Paillard et al.*, 1996] with a Bartlett-type window. To test the significance of the peaks we compared the high-resolution and the low-resolution spectra. Peaks from the high-resolution spectrum that rise above the low-resolution spectrum by a distance larger than the one-sided 80% confidence level were considered significant. The wavelet analysis was performed using the online interactive wavelet plot from University of Colorado (http://atoc.colorado.edu/research/wavelets) [*Torrence and Compo*, 1998]. We applied a Morlet wavelet basis function to the evenly resampled time series, assuming a red noise background spectrum and a significance level at 20% (80% confidence). Insolation time series were calculated using software AnalySeries 1.1 [*Paillard et al.*, 1996] at 10°N, applying the Laskar series for September (solar longitude = 180°) and February (solar longitude = 330°).

4. Results

4.1. Dinoflagellate Cyst Assemblages

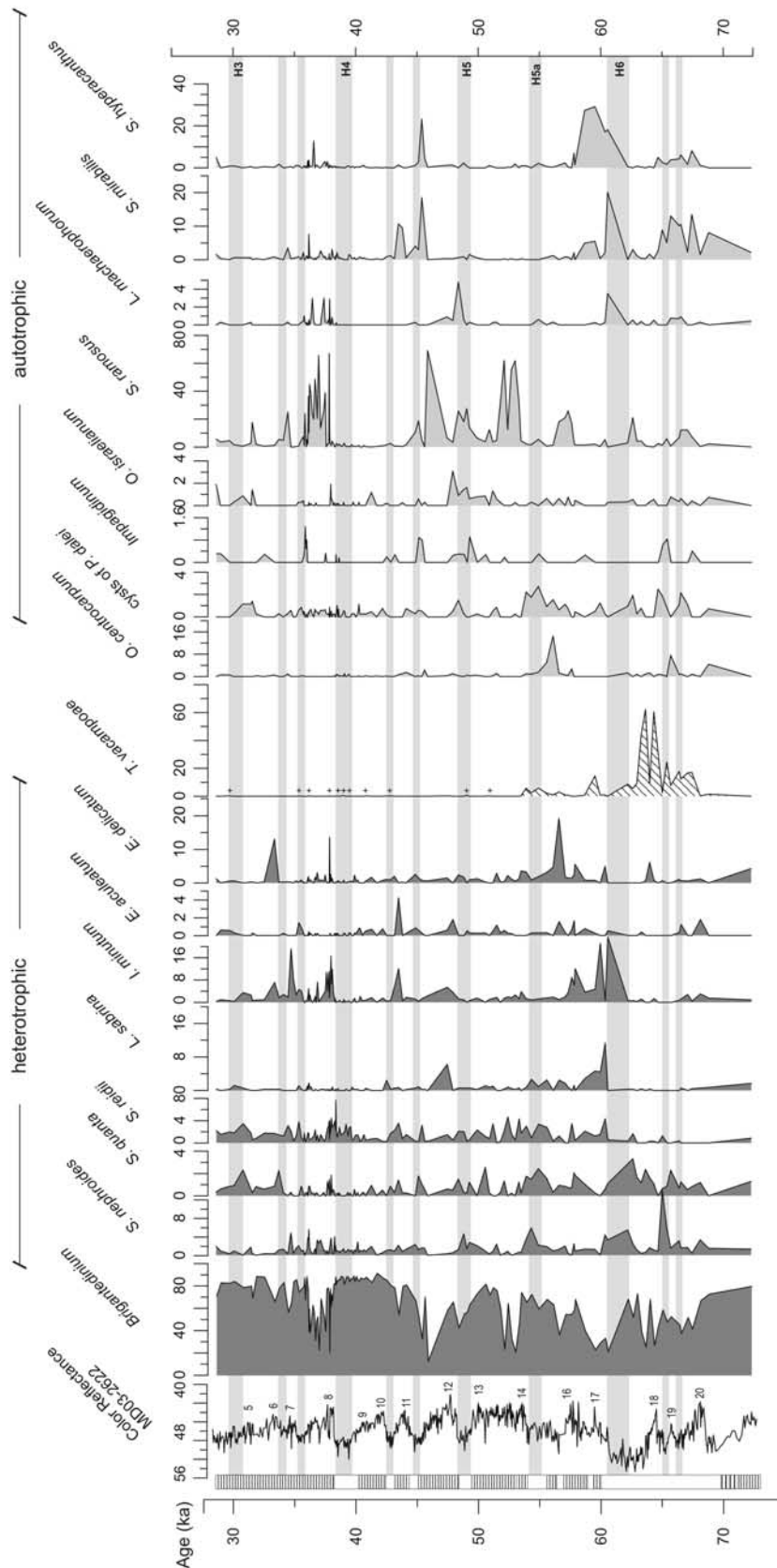[16] Core MD032-622 hosts a rich sedimentary record of organic-walled dinoflagellate cysts, pollen grains and

Figure 2. Relative abundances of main organic-walled dinoflagellate taxa expressed in percentages of total cysts from core MD03-2622. Reflectance curve (550 nm) and laminated intervals are indicated [*Løj*, 2004]. Maxima in the color reflectance curve correlated with the Greenland interstadials are numbered accordingly. Gray bars indicate Greenland stadials. Note the different percentage scales for different species.
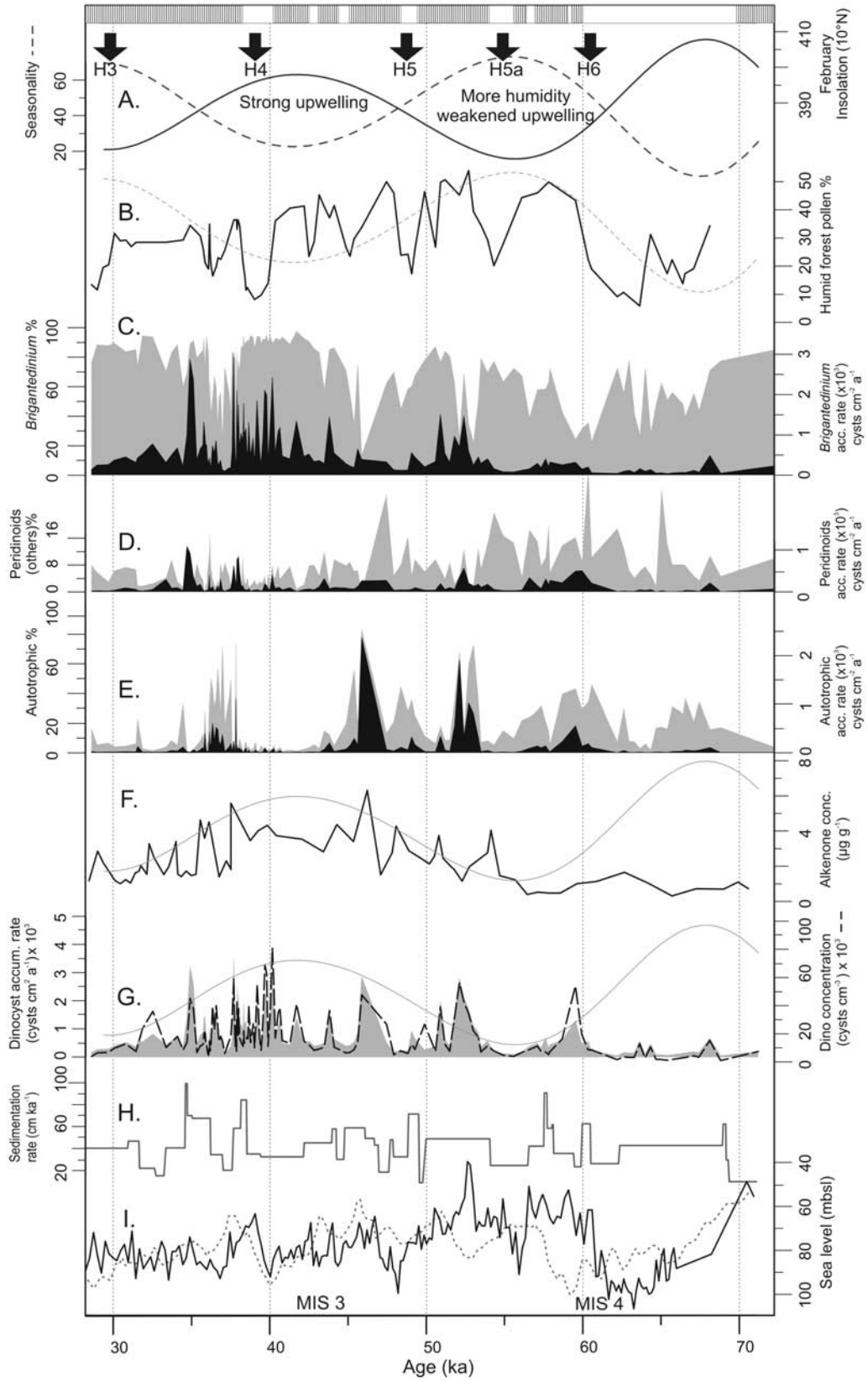
Figure 3

spores. Across the studied sequence of core MD03-2622 forty dinocyst taxa were identified (Table 1). The assemblages (Figure 2) are dominated by cysts of congruentidiacean heterotrophic species, mainly *Brigantedinium* spp. that are accompanied by *Echinidinium* spp., *Selenophemphix nephroides*, *S. quanta*, *Stelladinium reidii*, which generally dominate areas with enhanced nutrient conditions and active upwelling [*Marret and Zonneveld*, 2003]. Autotrophic cysts from the Gonyaulacales dominate the assemblage during four distinct periods (around 58, 53, 46, and 38 ka), in which *Spiniferites* species (*S. ramosus*, *S. mirabilis*, *S. hyperacanthus*) are accompanied by cysts of *Pentapharsodinium dalei*, *Operculodinium centrocarpum* sensu Wall and Dale, *Nematosphaeropsis labyrinthus* and *Lingulodinium machaerophorum*. The cyst species *Islandinium minutum,* previously described only from cold polar/subpolar waters, was found abundantly in our record together with the *Spiniferites* group. The coastal euryhaline cyst *Tuberculodinium vancampoae* dominates the oldest part of the record.

[17] The diversity structure of the dinoflagellate community seems to be influenced by the ratio between heterotrophic and autotrophic species. Heterotrophic dinocyst abundance and diversity show opposite trends, indicating a contrasted community structure along MIS 3 and MIS 4. Diversity does not show substantial stadial-interstadial variations, even if warm interstadials tend to maintain more diverse, autotrophic-dominated communities. More noticeable is the general decline toward less diverse communities toward the end of MIS 3, with a clear drop around 42 ka. Except for interstadial 8 (38.4–36.4 ka), which is clearly autotrophic-dominated, this last part of MIS 3 (42–29 ka) consists almost exclusively of heterotrophic dinocysts, mainly *Brigantedinium* spp.

4.2. Dinoflagellate Cyst Concentrations and Accumulation Rates

[18] Along the sampled sequence, concentrations of dinoflagellate cysts vary abruptly and repeatedly between <5000 and >80,000 cysts/cm^3 (Figure 3g). Accumulation rates and concentration values during MIS 4 are almost two orders of magnitude lower than during MIS 3. At millennial scales, high dinoflagellate cyst concentrations mainly coincide with warm interstadials, and low cyst concentrations with cold stadials, similar to pollen concentrations [*González et al.*, 2008]. High total accumulation rates of dinocysts in the Cariaco Basin range between ∼100 and ∼4000 cysts/cm^2/a (Figure 3g) and are comparable to other upwelling regions like the Santa Barbara Basin [*Pospelova et al.*, 2006] and the Arabian Sea [*Zonneveld and Brummer*, 2000; *Reichart and Brinkhuis*, 2003].

[19] Although total concentrations and accumulation rates of dinoflagellate cysts show to be concordant with the stadial-interstadial variability, a different pattern arises when comparing the accumulation rates of different groups. Rates of *Brigantedinium* are higher than those of autotrophic dinoflagellates, and show a clear maximum between 42 and 38 ka (Figures 3c and 3e). Autotrophic dinoflagellate cyst accumulation rates mainly consist of four distinct peaks between 36 and 60 ka (∼58, 53, 46 and 37 ka). Accumulation rates of most non-*Brigantedinium* heterotrophic dinocysts coincide with autotrophic maxima, supporting the observation that communities are more diverse during periods of *Brigantedinum* decline (Figures 3d and 3e).

[20] The B-T spectral analysis of total dinocyst accumulation rates indicates a trend of roughly 36–42 ka, which may be part of orbital variation. After subtracting the low-frequency trend, the total accumulation rates series showed significant (80%) periodicities of decreasing power at 6.2, 2.85, and 0.95 ka (Figures 4a and 4b). In order to better understand the consistency of these periodicities within different components of the dinocyst assemblage, we performed the B-T analysis by splitting the accumulation rates into three ecological groups: *Brigantedinium* spp., other Peridinoid cysts excluding *Brigantedinium* (henceforth called Peridinoids), and autotrophic cysts. In order to provide a more detailed identification of high-frequency periodicities original individual series were detrended by subtracting the low-frequency cubic trend.

[21] The spectral analysis showed the 7.5–6.7 ka periodicity to be significant for the autotrophic and Peridinoid series, and slightly below the significance level for the *Brigantedinium* series. The periodicities between 3.2 and 2.36 ka are shared by the autotrophic and Peridinoid series. Significant power in the 1.78 ka periodicity band was found for the *Brigantedinium* group. All three series showed significant periodicities between 1.2 and 0.8 ka (Figure 4).

[22] The results of the wavelet analysis confirm the periodicities, as described by B-T analysis, providing information on their temporal distribution. The oldest and the youngest sections of the record are characterized by the absence of clear cycles in all series. Between 62 and 40 ka the record is characterized by a ∼7 ka cycle, while higher frequencies appear to codominate the spectrum some thousand of years after, from 54 to 35 ka.

5. Discussion

[23] Dinoflagellates are important constituents of the marine phytoplankton community, and thus dinoflagellate

Figure 3. Down core variations of (a) February insolation in W/m^{2}and seasonality in W/m^2 at 10°N, (b) relative abundance expressed in percentages of total pollen and spores of forest pollen from core MD03-2622 [*González et al.*, 2008], (c) *Brigantedinium* cyst percentages of total cysts (gray shaded) and accumulation rates (black), (d) Peridinoid cyst percentages of total cysts (gray shaded) and accumulation rates (black), (e) autotrophic dinoflagellate cyst percentages of total cysts (gray shaded) and accumulation rates (black), (f) alkenone concentration from site ODP 1002 [*Herbert and Schuffert*, 2000], (g) total dinoflagellate cyst concentration (dotted line) and accumulation rates (shaded) from core MD03-2622, (h) sedimentation rates of core MD03-2622, and (i) sea level reconstructions from the Red Sea (solid line) [*Rohling et al.*, 2004] and northern Red Sea (dashed line) [*Arz et al.*, 2007]. On top, laminated intervals and timing of Heinrich events [*Hemming*, 2004; *Rashid et al.*, 2003] are denoted.

A. Total dinocyst accumulation rate

B.

C. *Brigantedinium* accumulation rate

D.

E. Peridinoid cysts (others) accumulation rate

F.

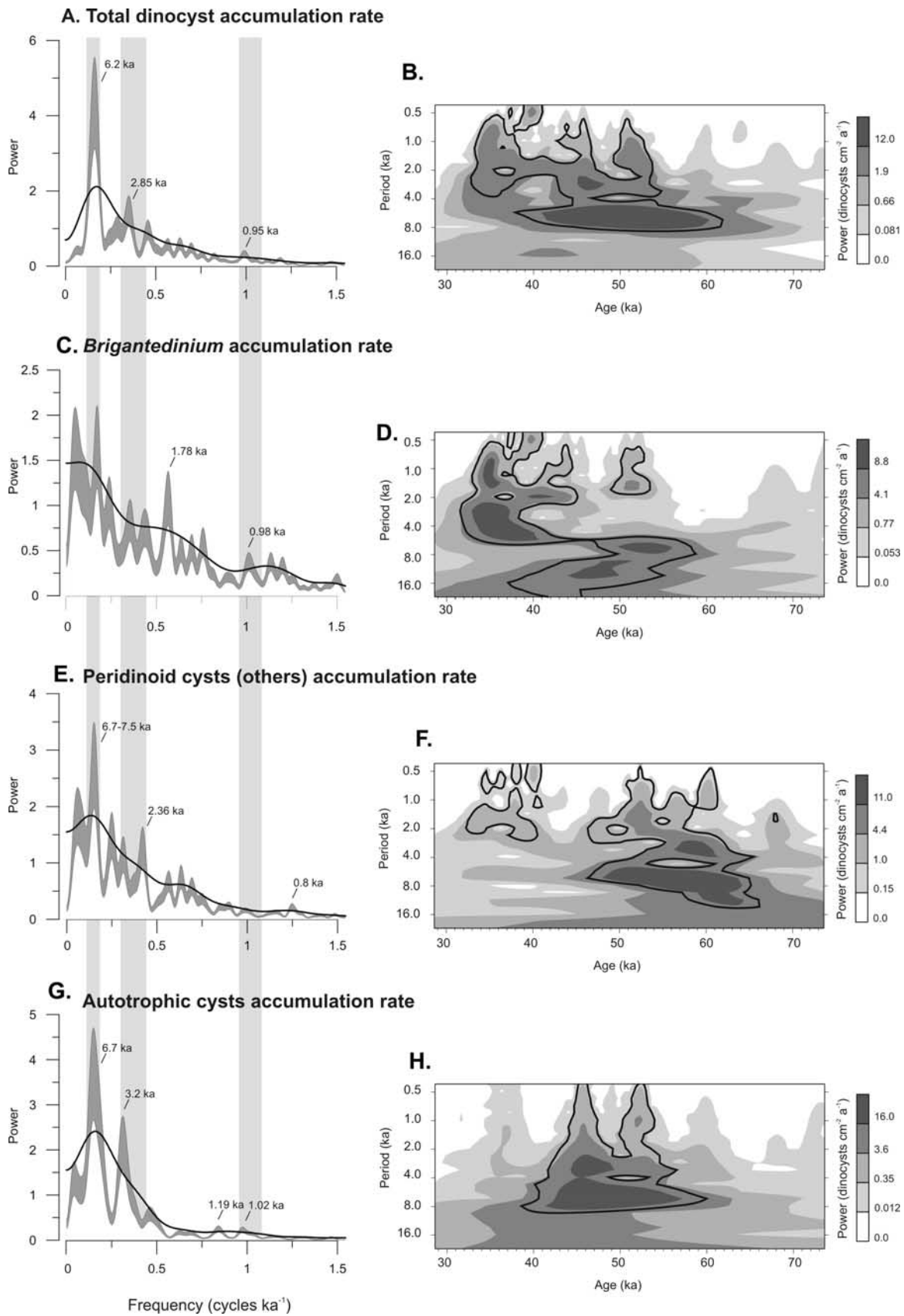**G. Autotrophic cysts accumulation rate**

H.

Figure 4

cyst accumulation rates are associated with marine productivity and export production. Dinocyst accumulation rates in the Cariaco Basin, in the order of over 4000 cysts/cm^2/a are typical of nutrient-rich and upwelling regions [e.g., *Zonneveld and Brummer*, 2000; *Reichart and Brinkhuis*, 2003; *Pospelova et al.*, 2006]. However, they showed high variability at different time scales suggesting changes in primary productivity and phytoplankton community structure during MIS 3 and MIS 4.

5.1. MIS 3/MIS 4 and Orbital-Scale Variability

[24] MIS 3 is characterized by higher concentration and accumulation rates of dinoflagellate cysts, contrasting with the very low cyst concentration and accumulation rates that characterize MIS 4 (Figure 3). Additionally, wavelet analysis showed no significant cycles during MIS 4 (see below). At orbital time scales, the heterotrophic (mainly *Brigantedinium*) accumulation rates opposed the autotrophic cyst accumulation rates, although the pattern is interrupted by stadial-interstadial variability. Alkenone concentration is an indicator of coccolithophorid export production that closely resembles the total organic carbon (TOC) variations in the basin [*Herbert and Schuffert*, 2000; *Haug et al.*, 1998]. Alkenone concentration from the nearby ODP 1002 core consistently shows the same pattern as observed in the total dinocyst concentration. Alkenone concentration might be considered a proxy for haptophyte production [*Goñi et al.*, 2003], since changes in sedimentation rates are not large enough to reshape the trends found on concentrations. Maximum dinoflagellate concentrations and accumulation rates around 38–48 ka coincide with maximum alkenone concentrations (Figure 3f), suggesting that recorded changes in dinoflagellate productivity are indeed reflecting changes in the phytoplankton community.

[25] Global sea level may have played a primary role in controlling the contrast of phytoplankton export production between MIS 4 and MIS 3. During low sea levels the Cariaco Basin was isolated from the open Caribbean by the shallower sills, restricting the import of nutrient-rich subsurface waters (i.e., Subtropical Underwater [cf. *Kameo et al.*, 2004]), and keeping the MIS 4 productivity levels below those of MIS 3. However, the intensity of upwelling-favorable winds during sea level highstands would have had an additional effect on the productivity intensity and the establishment of bottom water anoxia at shorter time scales.

[26] September is the month during which the ITCZ attains its northernmost position, and thus maximum rainfall in the Cariaco Basin matches September insolation [*Koutavas and Lynch-Stieglitz*, 2004]. In the same way maximum upwelling season matches February insolation. The difference between September insolation and February insolation at 10°N can be used as a measure of seasonality for the Cariaco Basin region (Figure 3a). In the Cariaco Basin heterotrophic dinocysts (mainly *Brigantedinium* spp.) accumulation rates show several maxima during the period with low September insolation (10°N) related to a broad period of minimum seasonality (38–47 ka). As *Brigantedinium* is considered a typical taxon representative of high nutrient conditions, high productivity and upwelling areas [*Dale and Fjellsa*, 1993; *Reichart and Brinkhuis*, 2003], the *Brigantedinium* accumulation maxima suggest an increment in the productivity signal related to the intensification of the upwelling season as a response to higher boreal winter insolation.

[27] Changes in the seasonal distribution of solar radiation on the precession cycle are known to exert a strong influence over tropical climates. Periods of reduced insolation seasonality at low latitudes have been recognized as periods of reduced or absent El Niño activity [*Koutavas et al.*, 2002]. Indeed, coral records from Papua New Guinea [*Tudhope et al.*, 2001] suggest reduced ENSO activity during the 38–42 ka period. Today, occasional lower phytoplankton production years may be associated with ENSO events [*Muller-Karger et al.*, 2004].Therefore, reduced ENSO activity induced by reduced insolation seasonality during the 38–42 ka period, may have strengthened the effects of maximum February (10°N) insolation, leading to enhanced upwelling in the Cariaco Basin. The absence of a peak in heterotrophic dinoflagellate productivity around 68 ka, when February insolation also reaches a maximum, remains unexplained. However, the lowered sea level (approximately ∼80 m) during MIS 4 might have exerted a stronger influence on nutrient availability and thus on marine productivity, which would obscure the potential response of phytoplankton to insolation forcing.

[28] During the 50–58 ka period low February (10°N) insolation promoted more humid conditions over the Basin and concurrently reduced upwelling. During the early part of MIS 3 a series of autotrophic dinoflagellate cyst accumulation maxima occurred (Figure 3e). Autotrophic dinoflagellates depend on the availability of light and nutrients, and since they do not feed on other plankton, they can easily compete for resources during the nonupwelling season. In fact, today the phytoplankton community during the nonupwelling season is autotrophic-dominated and very diverse compared to the upwelling season [*Ferraz-Reyes*, 1983].

Figure 4. Power spectra and wavelet analysis of the detrended and resampled time series of core MD03-2622: (a and b) total dinocyst accumulation rate, (c and d) *Brigantedinium* accumulation rate, (e and f) Peridinoid (excluding *Brigantedinium*) accumulation rate, and (g and h) autotrophic cyst accumulation rate. Figures 4a, 4c, 4e, and 4g show the results of the Blackman-Tuckey spectral analysis. The analyses were performed with a Barlett-type window. Those peaks of the high-resolution spectrum (filled with gray) that rise above the low-resolution spectrum (solid line) by a distance greater than the one-sided confidence interval at the 80% level (spectra filled with white) are considered to be significant [*Felis et al.*, 2000]. The wavelet power spectra, shown in Figures 4b, 4d, 4f, and 4h, were calculated using the Morlet wavelet [*Torrence and Compo*, 1998]. The contour levels are chosen so that 75%, 50%, 25%, and 5% of the wavelet power is above each level, respectively. The thick contour is the 80% confidence level using a red noise background. Gray bars highlight the main periodicity bands discussed in the text.
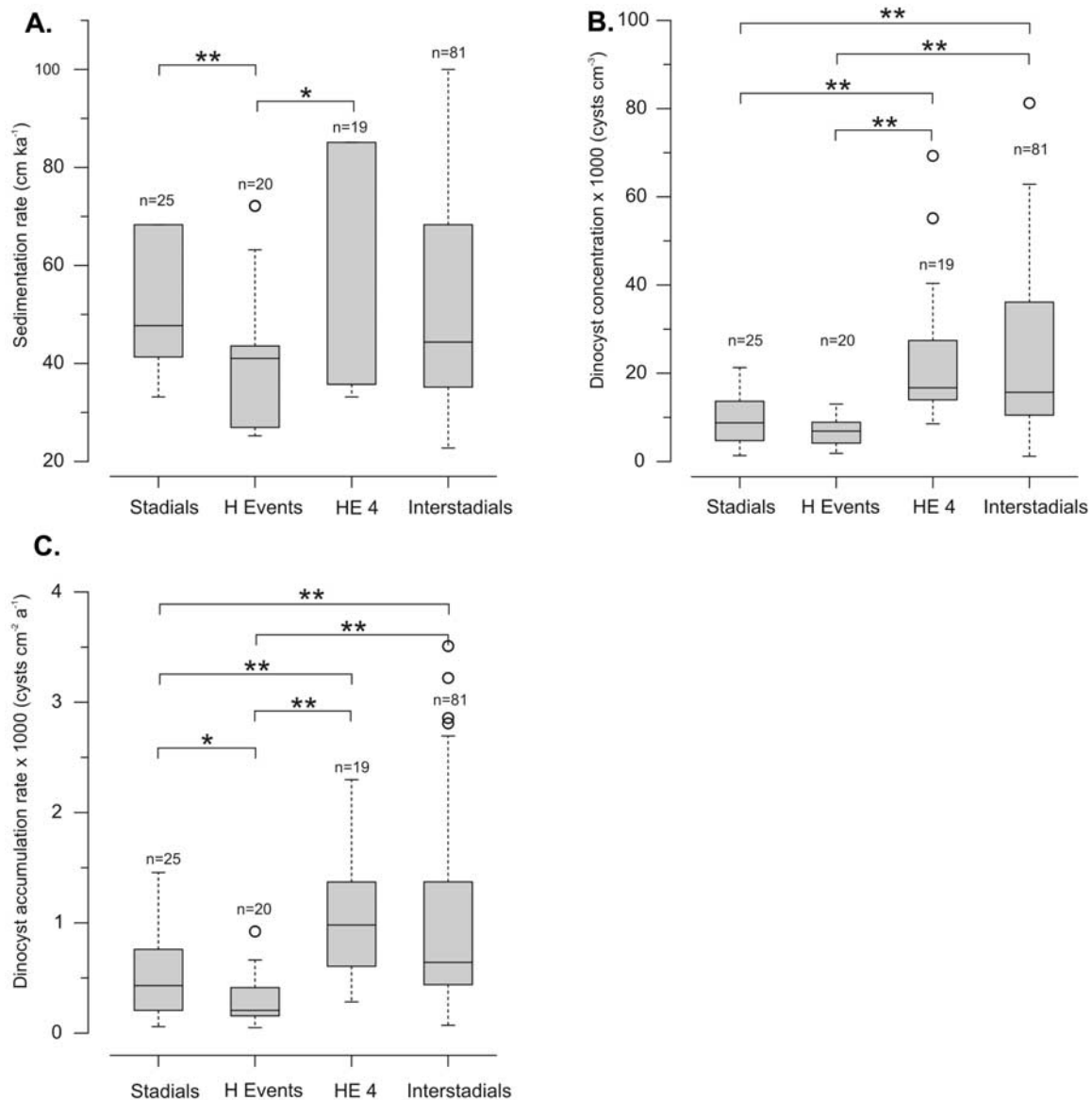
Figure 5. Box plot comparison of (a) sedimentation rates, (b) dinoflagellate cyst concentrations, and (c) dinoflagellate accumulation rates between stadials, HE stadials, HE 4 stadial, and interstadials. Concentrations and accumulation rates during interstadials showed to be significantly higher than during both stadials and HE stadials. Asterisk represents statistical significance (p < 0.05) by Student's *t* test, and double asterisk represents statistical significance (p < 0.01) by Student's *t* test.

Therefore, we use autotrophic cyst accumulation rates as indicators of a more stratified water column that coincide with rainy periods and fresher and warmer sea surface conditions. Similarly to what occurs at the seasonal scale, periods of high rainfall also result in higher inputs of terrestrial nutrients that lead to more diverse phytoplankton communities, favoring principally the development of rich coastal assemblages that benefit from the fluvial nutrient plume. During the 58–50 ka interval, high relative abundance of pollen from the humid forest corroborates the prevalence of more humid conditions over the continent [*González et al.*, 2008].

5.2. Millennial Time Scales

[29] During MIS 3 most warm interstadials in the Northern Hemisphere coincide with dark, laminated sediments deposited under anoxic bottom water conditions in the Cariaco Basin, and stadial periods coincide with light and bioturbated sediments. Considerable fluctuations in dinocysts accumulation rates and concentrations during MIS 3 are concurrent with these stadial-interstadial shifts, with values significantly higher occurring mainly during Northern Hemisphere interstadials, and lower rates during Northern Hemisphere stadials (Figures 3 and 5). One exception was found during H4, which showed concentrations and

accumulation rates higher than all the other stadial values, resembling more the interstadial situation. Differences in sedimentation rates between stadials and interstadials did not show to be statistically significant (Figure 5), meaning that the differences found on concentration, and thus in accumulation rates values between stadials and interstadials, truly reflect changes in productivity and are not the mere effect of dilution or concentration of sediments.

[30] Spectral analysis provides additional evidence of the influence that Northern Hemisphere millennial-scale changes exerted on the hydrology and productivity of equatorial regions. Indeed, the 3.2–2.85 ka periodicity identified in the total and autotrophic series (Figure 4) can be explained as multiples of the Dansgaard/Oeschger cycles, which occur with approximately 1500 year spacing [*Rahmstorf*, 2003], similar to what *Kaiser et al.* [2007] observed for the ODP 1002 reflectance time series.

[31] High productivities during MIS 3 interstadials resulting in high abundances of the foraminifer *Globigerina bulloides* in the laminated intervals and the high $CaCO_3$ accumulation rates [*Peterson et al.*, 1991, 2000a] are responsible for oxygen consumption and the establishment of anoxic depositional conditions in the basin, which is consistent with our high accumulation rates of dinocysts. Interstadials have been described as periods of greater rainfall and thus terrigenous input to Cariaco Basin, as reflected by the increase of forest pollen taxa and high Ti and Fe contents [*Peterson et al.*, 2000a; *Haug et al.*, 2001; *González et al.*, 2008]. Under this perspective, the observed higher dinoflagellate cyst accumulation rates during interstadials in the Cariaco Basin imply the occurrence of a clear rainy season characterized by relaxed vertical mixing, which favors the spreading of dinoflagellates in the phytoplankton community. More diverse and autotrophic-rich dinoflagellate assemblages during most interstadials, especially the interstadials following HEs, reinforce this view, since autotrophic-dominated assemblages flourish, as mentioned before, preferentially under stratified conditions promoted by higher fluvial discharge of warm and fresh waters.

[32] Rich coastal assemblages that benefit from the fluvial nutrient plume are particularly prolific, as is the case of some Peridinoid taxa like *Lejeunecysta* spp. and *Echinidinium delicatum* (Figure 2) that, unlike most other heterotrophic taxa, have been found associated with river outflow waters and stratified conditions [*Vink et al.*, 2000; *Holzwarth et al.*, 2007]. The good correspondence between autotrophic dinoflagellate cysts and Ti measurements, an indicator of fluvial input [*Peterson et al.*, 2000a], confirms the close relationship that exists between autotrophic taxa (mainly *Spiniferites ramosus*) and riverine runoff (Figure 6).

[33] Contrastingly, the significantly low cyst accumulation rates that characterize the light, bioturbated stadial sediments suggest either a sharp decrease in dinoflagellate productivity or a strong degradation effect caused by the prevalence of oxic conditions. If degradation was the main cause of cyst variability at millennial time scales, we should expect sharp declines of accumulation rates occurring only during periods of bioturbated sediment, but the record shows clear shifts between high and low accumulation rates even during laminated segments (e.g., 38–30 ka, 57–56 ka,

Figure 3). From the dinoflagellate assemblage there is no evidence of major degradation occurring during stadials, indicated by the high relative abundance (>80%) of Peridinoids, which are sensitive to degradation [*Zonneveld et al.*, 2007]. We therefore conclude that low accumulation rates during stadials are truly reflecting diminished productivity in the basin.

[34] Stronger upwelling in the Cariaco Basin is indeed expected during stadials according to the hypothesis of latitudinal migrations of the ITCZ following Greenland climate [*Peterson and Haug*, 2006]. A southward migration of the ITCZ has been proposed as the main mechanism driving hydrologic changes in northern South America during stadials and HEs, causing simultaneously dry conditions over the Cariaco Basin and wetter conditions over northern Brazil and Bolivia [*Arz et al.*, 1998; *Baker et al.*, 2001]. Intensified trade winds along the northern coast of Venezuela, would promote strong upwelling in the region. Some evidence from phytoplankton community reconstructions during the Younger Dryas period, suggests higher upwelling-related productivity, as the result of an intensified annual cycle during this cooler North Atlantic SST interval [*Hughen et al.*, 1996; *Peterson et al.*, 1991, 2000a; *Dahl et al.*, 2004].

[35] Although the migration of the ITCZ may account for the prevalence of a mixed water column during Northern Hemisphere cold stadials, the low cyst accumulation rates cannot be explained by this mechanism only. Millennial-scale variability in marine productivity requires a mechanism similar to glacial-interglacial variations that controls the supply of nutrients, and the alternation of anoxic-oxic bottom waters. Today, phytoplankton growth is sustained by seasonal upwelling of Subtropical Underwater (SUW) [*Scranton et al.*, 2006]. As the SUW enters the basin at an approximate depth of 150 m, it sinks and then rises again along the southeastern corner of the basin, bringing nutrients and dissolved organic carbon to the surface. During MIS 3, when sea level was ~70–100 m lower than at present [*Lambeck and Chappell*, 2001; *Siddall et al.*, 2003], the amount of SUW water entering the shallow sill basin might have been limited, restricting the general availability of nutrients. The rapid sea level changes that occurred during the longest stadials during MIS 3, estimated to be in the order of 15–35 m [*Siddall et al.*, 2003; *Rohling et al.*, 2004; *Arz et al.*, 2007], might have had an additional effect in modulating the nutrient availability during MIS 3 at millennial time scales. Furthermore, there is some evidence showing that the nutrient concentration of the SUW varied at glacial-interglacial scales, since the main supply of thermocline waters coming from the North Atlantic subtropical gyre changed drastically. Reconstructions of stable isotopes in benthic foraminifera from the Bahama Bank [*Slowey and Curry*, 1995], and coccolithophorid assemblages in the central Caribbean [*Kameo et al.*, 2004] both indicate a SUW depleted in nutrients during glacial intervals. Similarly, at millennial time scales, a Caribbean record of calcareous dinoflagellates from core M35003-4 shows regular excursions to extremely oligotrophic conditions during HEs [*Vink et al.*, 2001]. We therefore propose that the recorded low marine productivities in the Cariaco Basin
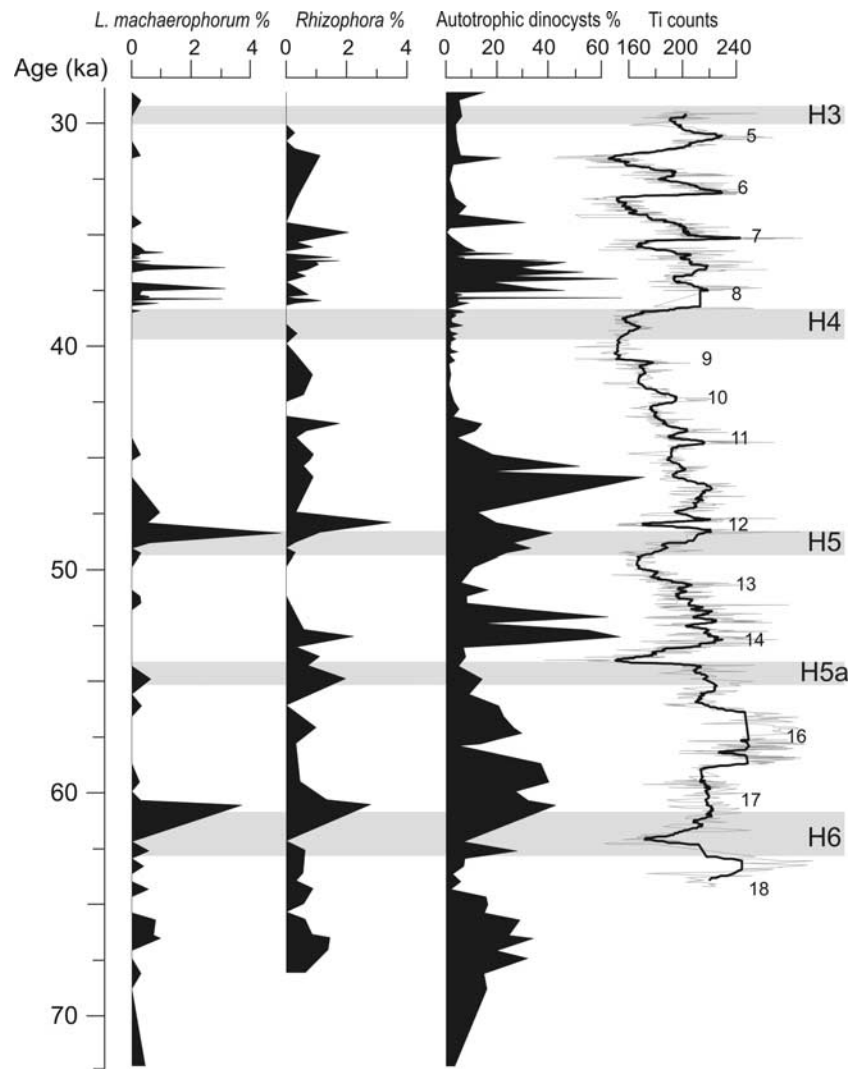
Figure 6. Comparison of the relative abundance of autotrophic dinocysts from core MD03-2622 with Titanium counts from the nearby core ODP 1002 [*Peterson et al.*, 2000a], a proxy for riverine runoff. Marine stratified surface conditions develop during periods of increased input of fresh and nutrient rich waters, especially after most prominent HE stadials. The *Lingulodinium machaerophorum* dinocyst percentages indicate enhanced fluvial input, while the *Rhizophora* (mangrove) pollen percentages suggest sea level change and enhanced fluvial input. Heinrich events (H3–H6) are denoted according to cited ages [*Rashid et al.*, 2003; *Hemming*, 2004], and interstadials are numbered as in ice core GISP2.

during stadials are related to the reduced inflow of a nutrient impoverished SUW that generally characterized glacial conditions. This situation was only interrupted by intermittent fluxes of terrestrial-derived nutrients during interstadials. Additionally, the southward displacement of the oligotrophic North Equatorial Current, might have exerted a strong influence in nutrient availability, especially during the most extreme stadials (namely HEs), as proposed by *Vink et al.* [2001].

[36] Summarizing, from the Cariaco Basin dinocyst record we infer that MIS 3 stadials were periods of active upwelling promoted by the strengthening of trade winds, but productivity probably has been lower than during interstadials (except for heterotrophic dinoflagellates) since

nutrient supply was strongly reduced. Contrastingly, interstadials were characterized by high dinoflagellate productivity supported by the enhanced supply of riverine nutrients (Figure 7).

[37] Superimposed to the mentioned Dansgaard/Oeschger cyclicity, we found evidence of higher-frequency periodicities identified by spectral analysis that cannot be attributed to this pattern. The significant 1.78 ka spectral peak found in the *Brigantedinium* time series (Figures 4c and 4d), and the ~1 ka cycle found in all dinoflagellate time series (Figure 4), suggest the existence of different mechanisms that simultaneously affect the upwelling intensity, and thus the productivity in the Cariaco Basin at millennial time scales. A well-defined 1800 year lunar cycle was already
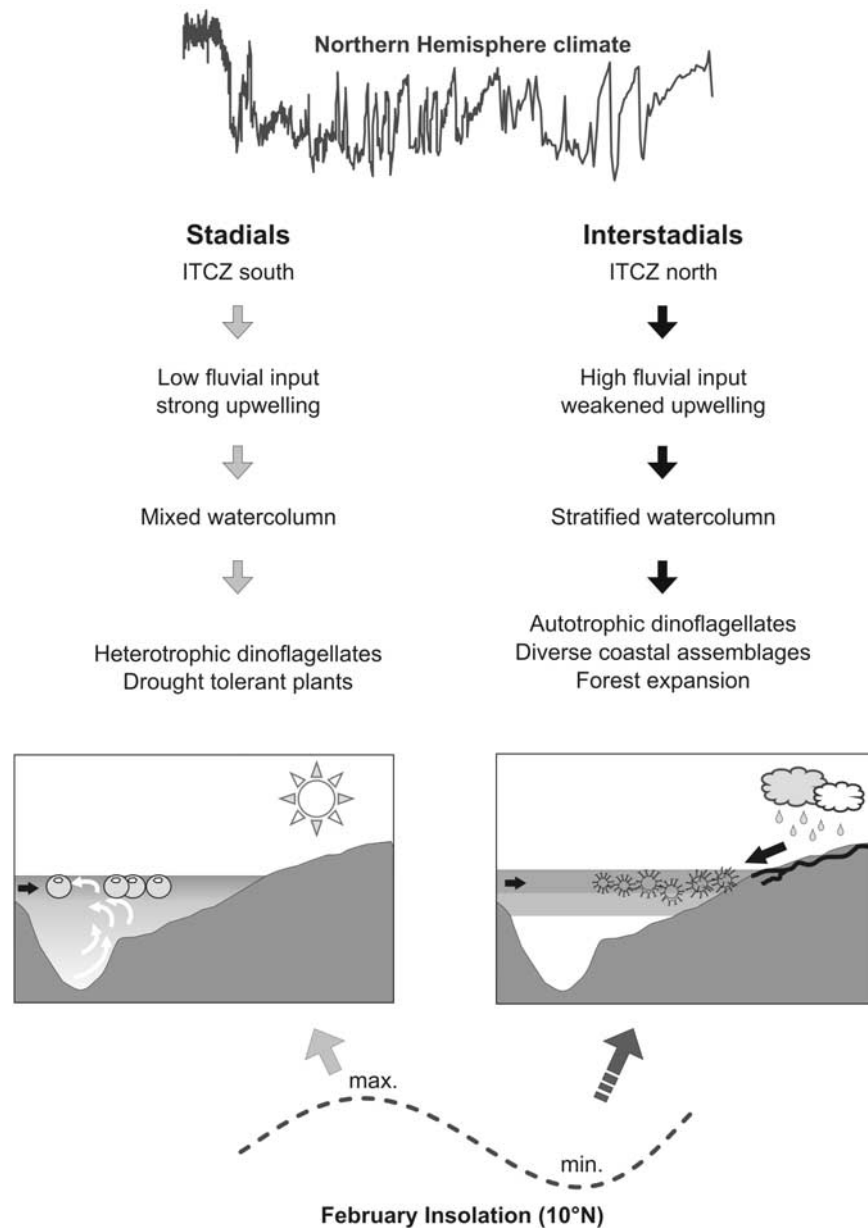
Figure 7. Schematic summary of main millennial productivity changes in the Cariaco Basin during MIS 3.

proposed as a plausible mechanism to explain suborbital variations in climate during the late Pleistocene [*Keeling and Whorf*, 2000], and it might potentially be related to the 1.78 ka cycle found in the Cariaco Basin record. Lunar cycles have a direct influence on the strength of oceanic tides and consequently on the intensity of vertical mixing, and therefore they have an effect on the phytoplankton community structure. The fact that *Brigantedinium*, an indicator of active upwelling and mixed waters, appears as the only group sensitive to this cyclicity, provide further support that lunar tidal cycles might be partially responsible for this variations in productivity. On the other hand, periodicities close to the 1 ka band have been revealed mainly for the Holocene by proxy records from, e.g., North Atlantic deep sediments [*Chapman and Shackleton*, 2000], Greenland δ^{18}O ice core records [*Schulz and Paul*, 2002] and Santa Barbara Basin sediments [*Nederbragt and Thurow*, 2005] as a response to solar intensity variations in the North Atlantic realm. It is beyond the scope of this study to discern whether these cycles recorded in tropical South America are related or not to North Atlantic climates. However, given the sensitivity of tropical atmospheric systems (e.g., ITCZ) to northern higher-latitude climates [*Haug et al.*, 2001; *Wang et al.*, 2004], it is likely that both periodicities are related to common forcing mechanisms.

5.3. Heinrich Events

[38] Heinrich events, even if not periodic, have shown a typical pacing of ∼7 ka [*Bond et al.*, 1993; *Broecker et al.*, 1992] during MIS 3. From the B-T and wavelet spectral analysis a periodicity of 6.7 ka was identified in the autotrophic dinocyst series that we relate to the HE recurrence. Major shifts in the dinocyst assemblage composition occurred during the interstadials that immediately followed after HEs (interstadials 17, 15–14, 12, and 8, Figures 2 and 3) and they are responsible for the 6.7 ka cyclicity mentioned above. These recurrent shifts to autotrophic-dominated assemblages show a regular increment of *Spiniferites ramosus*, *Lingulodinium machaerophorum*, accompanied by *Lejeunecysta* sp., and *Spiniferites mirabilis*. *Lingulodinium machaerophorum* is a good indicator of nutrient-rich and seasonally stratified waters typical of relaxed upwelling conditions [*Marret and Zonneveld*, 2003, and references therein]. *Spiniferites ramosus* is particularly abundant in stratified neritic environments under the influence of nutrient-rich river discharges [*Marret and Zonneveld*, 2003; *Wall et al.*, 1977; *Zonneveld et al.*, 2001]. We therefore infer that shortly after HE, stratified and eutrophic conditions prevailed in the Cariaco Basin. It is likely that during the transitions from oligotrophic mixed waters, characteristic of HEs, to interstadial conditions, short periods of high nutrient availability occurred, and relatively stratified waters persisted, because of a sudden increase in runoff and nutrient supply from the continent and the exposed shelf.

[39] Two other independent lines of evidence support the interpretation of enhanced runoff shortly after HEs. First, the Titanium record from the nearby ODP 1002 core (a proxy for riverine runoff) is in close correspondence with the variation of autotrophic dinoflagellates (Figure 6). Second, relative increments of *Rhizophora* (mangrove) pollen coincide with *L. machaerophorum* increments (Figure 6). Mangroves are known to be very sensitive to sea level and precipitation changes. Particularly in arid regions, as is the case of northern coastal Venezuela, mangrove distribution is strongly determined by groundwater salinity, hence by freshwater input, since hypersaline conditions are toxic to mangroves [*Cintrón et al.*, 1978; *Semeniuk*, 1983]. Consequently, the increments of *Rhizophora* pollen after hypersaline coastal environments during HEs [*González et al.*, 2008], indicate the prevalence of ameliorated, less saline conditions, promoted by enhanced freshwater availability.

Autotrophic dinoflagellates, mangrove pollen, and Titanium contents provide three convergent lines of evidence that support the idea of enhanced precipitation and riverine runoff shortly after HEs when interstadial climate conditions resumed.

6. Conclusions

[40] Organic-walled dinocysts from the Cariaco Basin are good indicators of paleoproductivity at different time scales. Both dinocyst assemblages and accumulation rates were sensitive to local insolation and global sea level changes at orbital (precessional) time scales, and to North Atlantic climate at millennial time scales. Differences between the more productive MIS 3 and the less productive MIS 4 were mainly determined by global sea level changes. During low sea levels the Cariaco Basin was largely isolated from the open Caribbean, and import of nutrient-rich waters was limited. During the 43–38 ka period of high February insolation (10°N), we identified higher upwelling-related productivity. Conversely, during the period 50–58 ka upwelling was weakened, and the continent was more humid. At millennial time scales, cyst accumulation rates shifted according to D/O variability. Although southward migrations of the ITCZ during stadials might be expected to drive strong upwelling, productivity during stadials was instead lower than during interstadials probably because nutrient supply from the open ocean and the land was much reduced (Figure 7). The most marked changes in eukaryotic productivity occurred shortly after HEs, when stratified and eutrophic conditions were established because of the sudden increase in runoff and nutrient supply from the continent and the exposed shelf.

References

Arz, H., J. Pätzold, and G. Wefer (1998), Correlated millennial-scale changes in surface hydrography and terrigenous sediment yield inferred from last-glacial marine deposits off northeastern Brazil, *Quat. Res.*, *50*, 157–166, doi:10.1006/qres.1998.1992.

Arz, H., F. Lamy, A. Ganopolski, N. Nowaczyk, and J. Pätzold (2007), Dominant Northern Hemisphere climate control over millennial-scale glacial sea-level variability, *Quat. Sci. Rev.*, *26*, 312–321, doi:10.1016/j.quascirev.2006.07.016.

Baker, P. A., C. A. Rigsby, G. O. Seltzer, S. C. Fritz, T. K. Lowensteink, N. P. Bacher, and C. Veliz (2001), Tropical climate changes at millennial and orbital timescales on the Bolivian Altiplano, *Nature*, *409*, 698–701, doi:10.1038/35055524.

Berger, W. H., M.-C. Bonneau, and F. L. Parker (1982), Foraminifera on the deep-sea floor: Lysocline and dissolution rate, *Oceanol. Acta*, *5*, 249–258.

Bond, G., et al. (1992), Evidence for massive discharges of icebergs into the North Atlantic ocean during the last glacial period, *Nature*, *360*, 245–249, doi:10.1038/360245a0.

Bond, G. C., W. S. Broecker, S. Johnsen, J. F. McManus, L. Labeyrie, J. Jouzel, and G. Bonani (1993), Correlation between climate records from North Atlantic sediments and Greenland ice, *Nature*, *365*, 143–147, doi:10.1038/365143a0.

Bond, G., W. Showers, M. Cheseby, R. Lotti, P. Almasi, P. deMenocal, P. Priore, H. Cullen, I. Hajdas, and G. Bonani (1997), A pervasive millennial-scale cycle in North Atlantic Holocene and glacial climates, *Science*, *278*, 1257–1266, doi:10.1126/science.278.5341.1257.

Broecker, W., G. Bond, M. Klas, E. Clark, and J. McManus (1992), Origin of the northern Atlantic's Heinrich events, *Clim. Dyn.*, *6*, 265–273, doi:10.1007/BF00193540.

Chapman, M. R., and N. J. Shackleton (2000), Evidence of 550-year and 1000-year cyclicities in North Atlantic circulation patterns during the Holocene, *Holocene*, *10*(3), 287–291, doi:10.1191/095968300671253196.

Cintrón, G., A. E. Lugo, D. J. Pool, and G. Morris (1978), Mangroves of arid environments in Puerto Rico and adjacent islands, *Biotropica*, *10*, 110–121.

Clayton, T., R. B. Pearce, and L. Peterson (1999), Indirect climatic control of the clay mineral composition of Quaternary sediments from the Cariaco basin, northern Venezuela (ODP site 1002), *Mar. Geol.*, *161*, 191–206, doi:10.1016/S0025-3227(99)00036-5.

Dahl, K. A., D. J. Repeta, and R. Goericke (2004), Reconstructing the phytoplankton community of the Cariaco Basin during the Younger Dryas cold event using chlorin steryl esters, *Paleoceanography*, *19*, PA1006, doi:10.1029/2003PA000907.

Dale, B., and A. Fjellsa (1993), Dinoflagellate cysts as paleoproductivity indicators: State of the art, potential, and limits, in *Carbon Cycling in the Glacial Ocean: Constraints on the Ocean's Role in Global Change: Quantitative Approaches in Paleoceanography*, NATO ASI Ser., Ser. I, vol. 17, edited by R. Zahn et al., pp. 521–537, Springer, Berlin.

Dansgaard, W., et al. (1993), Evidence for general instability of past climate from a 250-kyr ice-core record, *Nature*, *364*, 218–220, doi:10.1038/364218a0.

de Vernal, A., et al. (2001), Dinoflagellate cyst assemblages as tracers of sea-surface conditions in the northern North Atlantic, Arctic and sub-arctic seas: The new "n = 677" database and application for quantitative paleoceanographical reconstruction, *J. Quat. Sci.*, *16*, 681–699, doi:10.1002/jqs.659.

Felis, T., J. Pätzold, Y. Loya, M. Fine, A. H. Nawar, and G. Wefer (2000), A coral oxygen isotope record from the northern Red Sea documenting NAO, ENSO, and North Pacific teleconnections on Middle East climate variability since the year 1750, *Paleoceanography*, *15*(6), 679–694, doi:10.1029/1999PA000477.

Ferraz-Reyes, E. (1983), Estudio del fitoplancton en la Cuenca Tuy-Cariaco, Venezuela, *Bol. Inst. Oceanogr. Venezuela Univ. Oriente*, *22*(1–2), 111–124.

Giannini, A., Y. Kushnir, and M. A. Cane (2000), Interannual variability of Caribbean rainfall, ENSO, and the Atlantic Ocean, *J. Clim.*, *13*, 297–311, doi:10.1175/1520-0442(2000)013<0297:IVOCRE>2.0.CO;2.

Giannini, A., J. C. H. Chiang, M. A. Cane, Y. Kushnir, and R. Seager (2001), The ENSO teleconnection to the tropical Atlantic ocean: Contributions of the remote and local SSTs to rainfall variability in the Tropical Americas, *J. Clim.*, *14*, 4530–4544, doi:10.1175/1520-0442(2001)014<4530:TETTTT>2.0.CO;2.

Goñi, M., H. Aceves, R. C. Thunell, E. Tappa, D. Black, Y. Astor, R. Varela, and F. Muller-Karger (2003), Biogenic fluxes in the Cariaco Basin: A combined study of sinking particulates and underlying sediments, *Deep Sea Res., Part I*, *50*, 781–807, doi:10.1016/S0967-0637(03)00060-8.

González, C., L. M. Dupont, H. Behling, and G. Wefer (2008), Neotropical vegetation response to rapid climate changes during the last glacial: Palynological evidence from the Cariaco Basin, *Quat. Res.*, *69*, 217–230, doi:10.1016/j.yqres.2007.12.001.

Gordon, A. L. (1967), Circulation of the Caribbean Sea, *J. Geophys. Res.*, *72*, 6207–6223, doi:10.1029/JZ072i024p06207.

Haug, G., T. F. Pedersen, D. M. Sigman, S. E. Clavert, B. Nielsen, and L. Peterson (1998), Glacial/interglacial variations in production and nitrogen fixation in the Cariaco Basin during the last 580 kyr, *Paleoceanography*, *13*, 427–432, doi:10.1029/98PA01976.

Haug, G., K. Hughen, D. Sigman, L. Peterson, and U. Röhl (2001), Southward migration of the Intertropical Convergence Zone through the Holocene, *Science*, *293*, 1304–1308, doi:10.1126/science.1059725.

Hemming, S. (2004), Heinrich events: Massive late Pleistocene detritus layers of the North Atlantic and their Global Climate imprint, *Rev. Geophys.*, *42*, RG1005, doi:10.1029/2003RG000128.

Herbert, T. D., and J. D. Schuffert (2000), History of sea surface temperature variations in Cariaco Basin over a full glacial-interglacial cycle, *Proc. Ocean Drill. Program Sci. Results*, *165*, 239–247.

Holzwarth, U., O. Esper, and K. Zonneveld (2007), Distribution of organic-walled dinoflagellate cysts in shelf surface sediments of the Benguela upwelling system in relationship to environmental conditions, *Mar. Micropaleontol.*, *64*, 91–119, doi:10.1016/j.marmicro.2007.04.001.

Hughen, K. A., J. T. Overpeck, L. C. Peterson, and S. Trumbore (1996), Rapid climate changes in the tropical Atlantic region during the last deglaciation, *Nature*, *380*, 51–54, doi:10.1038/380051a0.

Hughen, K., S. Lehman, J. Southon, J. Overpeck, O. Marchal, C. Herring, and J. Turnbull (2004a), ^{14}C Activity and global carbon cycle changes over the past 50000 years, *Science*, *303*, 202–207, doi:10.1126/science.1090300.

Hughen, K., T. Eglinton, L. Xu, and M. Makou (2004b), Abrupt tropical vegetation response to rapid climate changes, *Science*, *304*, 1955–1959, doi:10.1126/science.1092995.

Hughen, K., J. Southon, S. Lehman, C. Bertrand, and J. Turnbull (2006), Marine-derived ^{14}C calibration and activity record for the past 50000 years updated from the Cariaco Basin, *Quat. Sci. Rev.*, *25*, 3216–3227.

Kaiser, J., F. Lamy, H. W. Arz, and D. Hebbeln (2007), Dynamics of the millennial-scale sea surface temperature and Patagonian Ice Sheet fluctuations in southern Chile during the last 70 kyr (ODP Site 1233), *Quat. Int.*, *161*, 77–89, doi:10.1016/j.quaint.2006.10.024.

Kameo, K., M. Shearer, A. W. Droxler, I. Mita, R. Watanabe, and T. Sato (2004), Glacial–interglacial surface water variations in the Caribbean Sea during the last 300 ky based on calcareous nannofossil analysis, *Palaeogeogr. Palaeoclimatol. Palaeoecol.*, *212*, 65–76.

Keeling, C. D., and T. Whorf (2000), The 1800-year oceanic tidal cycle: A possible cause of rapid climate change, *Proc. Natl. Acad. Sci. U. S. A.*, *97*(8), 3814–3819, doi:10.1073/pnas.070047197.

Koutavas, A., and J. Lynch-Stieglitz (2004), Variability of the marine ITCZ over the eastern Pacific during the past 30000 years: Regional perspective and global context, in *The Hadley Circulation: Present, Past and Future*, edited by R. S. Bradley and H. F. Diaz, pp. 347–369, Kluwer Acad., Dordrecht, Netherlands.

Koutavas, A., J. Lynch-Stieglitz, T. M. Marchitto Jr., and J.P. Sachs (2002), El Niño–like pattern

in ice age tropical Pacific sea surface temperature, *Science*, *297*, 226–230, doi:10.1126/science.1072376.

Laj, C. (2004), Cruise report: MD 132–P. I. C. A. S. S. O. images XI, Fortaleza-Baltimore-Brest, Mai Juin 2003, 53 pp., Inst. Polaire Fr. Paul Emile Victor, Plouzané, France.

Lambeck, K., and J. Chappell (2001), Sea level change through the last glacial cycle, *Science*, *292*, 679–686, doi:10.1126/science.1059549.

Maher, L. J., Jr. (1981), Statistics for microfossil concentration measurements employing samples spiked with marker grains, *Rev. Palaeobot. Palynol.*, *32*, 153–191, doi:10.1016/0034-6667(81)90002-6.

Marret, F., and K. Zonneveld (2003), Atlas of modern organic-walled dinoflagellate cyst distribution, *Rev. Palaeobot. Palynol.*, *125*, 1–200.

Martinez, J. I., G. Mora, and T. T. Barrows (2007), Paleoceanographic conditions in the western Caribbean Sea for the last 560 kyr as inferred from planktonic foraminifera, *Mar. Micropaleontol.*, *64*, 177–188, doi:10.1016/j.marmicro.2007.04.004.

Martinez, N. C., R. W. Murray, R. C. Thunell, L. C. Peterson, F. Muller-Karger, Y. Astor, and R. Varela (2007), Modern climate forcing of terrigenous deposition in the tropics (Cariaco Basin, Venezuela), *Earth Planet. Sci. Lett.*, *264*, 438–451, doi:10.1016/j.epsl.2007.10.002.

Metcalf, W. G. (1976), Caribbean-Atlantic water exchange through the Anegada-Jungfern passage, *J. Geophys. Res.*, *81*, 6401–6409, doi:10.1029/JC081i036p06401.

Mooers, C. N. K., and G. A. Maul (1998), Intra-Americas Sea circulation, in *The Sea*, 11th ed., edited by A. R. Robinson and K. H. Brink, pp. 183–208, John Wiley, New York.

Muller-Karger, F. E., et al. (2001), Annual cycle of primary production in the Cariaco Basin: Response to upwelling and implications for vertical export, *J. Geophys. Res.*, *106*(C3), 4527–4542, doi:10.1029/1999JC000291.

Muller-Karger, F., R. Varela, R. Thunell, Y. Astor, H. Zhang, R. Luerssen, and C. Hu (2004), Processes of coastal upwelling and carbon flux in the Cariaco Basin, *Deep Sea Res., Part II*, *51*, 927–943.

Nederbragt, A., and J. Thurow (2005), Amplitude of ENSO cycles in the Santa Barbara Basin, off California, during the past 15 000 years, *J. Quat. Sci.*, *20*(5), 447–456, doi:10.1002/jqs.946.

Paillard, D., L. Labeyrie, and P. Yiou (1996), Macintosh program performs time-series analysis, *Eos Trans. AGU*, *77*, 379, doi:10.1029/96EO00259.

Parsons, T. R., M. Takahashi, and B. Hargrave (1984), *Biological Oceanographic Processes*, 3rd ed., 330 pp., Pergamon, Oxford, U. K.

Peterson, L. C., and G. H. Haug (2006), Variability in the mean latitude of the Atlantic Intertropical Convergence Zone as recorded by riverine input of sediments to the Cariaco Basin (Venezuela), *Palaeogeogr. Palaeoclimatol. Palaeoecol.*, *234*, 97–113, doi:10.1016/j.palaeo.2005.10.021.

Peterson, L., J. T. Overpeck, N. G. Kipp, J. Imbrie, and D. Rind (1991), A high resolution late Quaternary upwelling record from the anoxic Cariaco Basin, Venezuela, *Paleoceanography*, *6*, 99–119, doi:10.1029/90PA02497.

Peterson, L., G. Haug, K. Hughen, and U. Röhl (2000a), Rapid changes in the hydrologic cycle of the tropical Atlantic during the Last Glacial, *Science*, *290*, 1947–1951, doi:10.1126/science.290.5498.1947.

Peterson, L. C., G. H. Haug, R. W. Murray, K. M. Yarincik, J. W. King, T. J. Bralower, K. Kameo, S. D. Rutherford, and R. B. Pearce (2000b), Late Quaternary stratigraphy and sedimentation at ODP Site 1002, Cariaco Basin (Venezuela), *Proc. Ocean Drill. Program Sci. Results*, *165*, 85–99.

Pospelova, V., T. F. Pedersen, and A. de Vernal (2006), Dinoflagellate cysts as indicators of climatic and oceanographic changes during the past 40 kyr in the Santa Barbara Basin, southern California, *Paleoceanography*, *21*, PA2010, doi:10.1029/2005PA001251.

Prospero, J. M., and P. J. Lamb (2003), African droughts and dust transport to the Caribbean: Climate change implications, *Science*, *302*, 1024–1027, doi:10.1126/science.1089915.

Rahmstorf, S. (2003), Timing of abrupt climate change: A precise clock, *Geophys. Res. Lett.*, *30*(10), 1510, doi:10.1029/2003GL017115.

Rashid, H., R. Hesse, and D. J. W. Piper (2003), Evidence for an additional Heinrich event between H5 and H6 in the Labrador Sea, *Paleoceanography*, *18*(4), 1077, doi:10.1029/2003PA000913.

Reichart, G.-J., and H. Brinkhuis (2003), Late Quaternary Protoperidinium cysts as indicators of paleoproductivity in the northern Arabian Sea, *Mar. Micropaleontol.*, *49*(4), 303–315, doi:10.1016/S0377-8398(03)00050-1.

Rochon, A., A. de Vernal, J.-L. Turon, J. Matthiessen, and M. Head (1999), Distribution of recent dinoflagellate cysts in surface sediments from the North Atlantic Ocean and adjacent seas in relation to sea-surface parameters, *Contrib. Ser.*, *35*, 59 pp., Am. Assoc. of Stratigr. Palynol. Found., College Station, Tex.

Rohling, E. J., R. Marsh, N. C. Wells, M. Siddall, and N. Edwards (2004), Similar melt-water contributions to glacial sea-level variability from Antarctic and northern ice sheets, *Nature*, *430*, 1016–1021, doi:10.1038/nature02859.

Schmidt, M. W., H. J. Spero, and D. W. Lea (2004), Links between salinity variation in the Caribbean and North Atlantic thermohaline circulation, *Nature*, *428*, 160–163, doi:10.1038/nature02346.

Schulz, M., and A. Paul (2002), Holocene climate variability on centennial-to-millennial time scales: 1. Climate records from the North Atlantic realm, in *Climate Development and History of the North Atlantic Realm*, edited by G. Wefer et al., pp. 41–54, Springer, Berlin.

Scranton, M. I., M. McIntyre, Y. Astor, G. T. Taylor, F. Muller-Karger, and K. Fanning (2006), Temporal variability in the nutrient chemistry of the Cariaco Basin, in *Past and Present Water Column Anoxia*, part II, *NATO Sci. Ser., IV*, vol. 64, pp. 139–160, edited by L. N. Neretin, Springer, Dordrecht, Netherlands.

Semeniuk, V. (1983), Mangrove distribution in northwestern Australia in relationship to regional and local freshwater seepage, *Vegetatio*, *53*, 11–31.

Siddall, M., E. J. Rohling, A. Almogi-Labin, D. Ch. Hemleben, I. Melschner, I. Schmelzer, and D. A. Smeed (2003), Sea-level fluctuations during the last glacial cycle, *Nature*, *423*, 853–858, doi:10.1038/nature01690.

Slowey, N. C., and W. B. Curry (1995), Glacial-interglacial differences in circulation and carbon cycling within the upper western North Atlantic, *Paleoceanography*, *10*(4), 715–732, doi:10.1029/95PA01166.

Torrence, C., and G. P. Compo (1998), A practical guide to wavelet analysis, *Bull. Am. Meteorol. Soc.*, *79*, 61–78, doi:10.1175/1520-0477(1998)079<0061:APGTWA>2.0.CO;2.

Tudhope, A. W., C. P. Chilcott, M. T. McCulloch, E. R. Cook, J. Chappell, R. M. Ellam, D. W. Lea, J. M. Lough, and G. M. Shimmield (2001), Variability in the El Niño–Southern Oscillation through a glacial-interglacial cycle, *Science*, *291*, 1511–1517, doi:10.1126/science.1057969.

Vink, A., K. A. F. Zonneveld, and H. Willems (2000), Organic-walled dinoflagellate cysts in western equatorial Atlantic surface sediments: Distributions and their relation to environment, *Rev. Palaeobot. Palynol.*, *112*, 247–286, doi:10.1016/S0034-6667(00)00046-4.

Vink, A., C. Rühlemann, K. Zonneveld, S. Mulitza, M. Hüls, and H. Willems (2001), Shifts in the position of the North Equatorial current and rapid productivity changes in the western tropical Atlantic during the last glacial, *Paleoceanography*, *16*, 479–490, doi:10.1029/2000PA000582.

Wall, D., B. Dale, L. P. Lohmann, and W. K. Smith (1977), The environmental and climatic distribution of dinoflagellate cysts in modern marine sediments from regions in the north and south Atlantic oceans and adjacent seas, *Mar. Micropaleontol.*, *2*, 121–200, doi:10.1016/0377-8398(77)90008-1.

Wang, X., A. S. Auler, R. L. Edwards, H. Cheng, P. S. Cristalli, P. L. Smart, D. A. Richards, and C. C. Shen (2004), Wet periods in northeastern Brazil over the past 210 kyr linked to distant climate anomalies, *Nature*, *432*, 740–743, doi:10.1038/nature03067.

Wang, Y. J., H. Cheng, R. L. Edwards, Z. S. An, J. Y. Wu, C.-C. Shen, and J. A. Dorale (2001), A high-resolution absolute-dated late Pleistocene monsoon record from Hulu Cave, China, *Science*, *294*, 2345–2348, doi:10.1126/science.1064618.

Werne, J. P., D. J. Hollander, T. W. Lyons, and L. C. Peterson (2000), Climate-induced variations in productivity and planktonic ecosystem structure from the Younger Dryas to Holocene in the Cariaco Basin, Venezuela, *Paleoceanography*, *15*, 19–29, doi:10.1029/1998PA000354.

Yarincik, K. M., R. W. Murray, and L. C. Peterson (2000), Climatically sensitive eolian and hemipelagic deposition in the Cariaco Basin, Venezuela, over the past 578000 years: Results from Al/Ti and K/Al, *Paleoceanography*, *15*, 210–228, doi:10.1029/1999PA900048.

Zonneveld, K. A. F., and G. A. Brummer (2000), Ecological significance, transport and preservation of organic walled dinoflagellate cysts in the Somali Basin, NW Arabian Sea, *Deep Sea Res., Part II*, *47*, 2229–2256, doi:10.1016/S0967-0645(00)00023-0.

Zonneveld, K. A. F., R. Hoek, H. Brinkhuis, and H. Willems (2001), Lateral distribution of organic walled dinoflagellates in surface sediments of the Benguela upwelling region, *Prog. Oceanogr.*, *48*, 25–72, doi:10.1016/S0079-6611(00)00047-1.

Zonneveld, K. A. F., F. Bockelmann, and U. Holzwarth (2007), Selective preservation of organic-walled dinoflagellate cysts as a tool to quantify past net primary production and bottom water oxygen concentrations, *Mar. Geol.*, *237*, 109–126, doi:10.1016/j.margeo.2006.10.023.

―――――――――――
L. M. Dupont, C. González, and G. Wefer, MARUM, University of Bremen, Leobener Strasse, D-28359 Bremen, Germany. (dupont@uni-bremen.de; catalina@uni-bremen.de; gwefer@marum.de)

K. Mertens, Research Unit Palaeontology, Department of Geology and Soil Science, Ghent University, S8, Krijgslaan 281, B-9000 Ghent, Belgium. (kenneth.mertens@ugent.be)